NEW METHOD FOR THE DESIGN AND THE SETTING UP PROCEDURE OF FILTERPLEXERS IN TELEVISION TRANSMITTERS

By

P. FERENCZY and P. SZALAI

Institute for Wireless Telecommunications Polytechnical University Budapest
and Electromechanical Laboratories Budapest

(Received April 20, 1961)

Presented by Prof Dr. I. BARTA

1. Introduction

The possibility of having the same antenna system for both the picture and sound transmitters is provided by the diplexer. Its task is — while providing the necessary good matching — to join together the outputs of the picture and sound transmitters, so that they should not appreciably interfere with each other.

At the same time it is necessary to attenuate the lower side-band of the amplitude modulated picture transmitter in order for the radiated spectrum to meet with international specifications. This makes it necessary to use a vestigial side-band filter between the antenna and the output of the picture transmitter.

There are several solutions of this twin problem in the literature [1, 2, 3]. One of these, that is most often used, is called the filterplexer, which is a combination of the diplexer and the vestigial side-band filter. The following discussion will concentrate on this version only.

The schematic circuit of the filterplexer with lumped elements is shown on Fig. 1. It consists essentially of two balun transformers for the input and output terminals, and of the reactive filter lines positioned symmetrically on two lines. The picture transmitter is connected to point A, so the voltages at points C and D will be of opposite phase, while point B remains at zero potential because of the symmetry.

The lengths of the coaxial lines from points C to L, and from D to M resp. are equal. All those frequency components coming from the picture transmitter, the frequencies of which fall in the pass band, will propagate through these lines and will be out of phase at points L and M, too. Because of the symmetry, this voltage will reach the antenna, connected to point J, while K will remain at zero potential.

If, however, there are such frequency components coming from the picture transmitter, which fall into the reject band, then these will be reflected by the filters connected parallel to the line at points E, F, G, and E', F', G' resp. Since the two filter lines are displaced by a quarter wavelength difference to each other, the reflected waves will be of the same phase, when they reach points C and D. This reflected power will produce voltage only at point B, while point A, *i.e.* the picture input, will get no power at all. The power appearing at point B will be dissipated by a resistor connected to this point.

The output of the sound transmitter is connected to point K. Because of the symmetry voltages of the same phase will appear at points L and M,

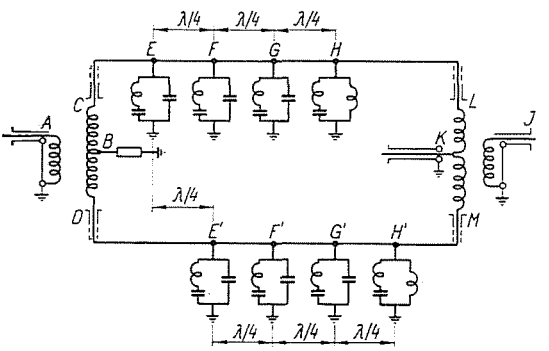

Fig. 1. The schematic, substituting circuit of the filterplexer

point J now remains at zero potential. Since the difference between line sections $H-L$ and $H'-M$ is exactly a quarter wavelength, the signals reaching H and H' resp. will be 90° in phase to each other. These two filters can be regarded as short circuits for the sound carrier and its side-bands, therefore they cause total reflection. The two reflected waves at L and M will now be exactly out of phase, since the waves pass twice through the quarter wavelength line section. This signal can get to the antenna without difficulty at point J. That fraction of a power coming from the sound transmitter, which was not reflected at filters H and H', will get to points C and D in phase, and so reaching the resistor at point B, will be dissipated.

It is quite clear by now, that no power can get either from the picture transmitter to the sound one or vica versa, while the powers of both transmitters reach the antenna. On the other hand the power of the rejected side band gets to a dissipating resistor, called the ballast resistor, designed especially for this purpose. This ballast resistor secures for the picture transmitter the constant input impedance throughout the rejected sideband.

The filterplexer is sometimes referred to as the bridge diplexer, because its working principle is somewhat analogous to AC bridges.

2. The design of the filterplexer for a given amplitude-frequency response

2.1 *The response curve from picture transmitter to aerial*

The international television organisations (OIRT, CCIR) prescribe the amplitude response of the radiated television signal. Our aim is to fulfil this specification. The requirements are schematically shown on Fig. 2.

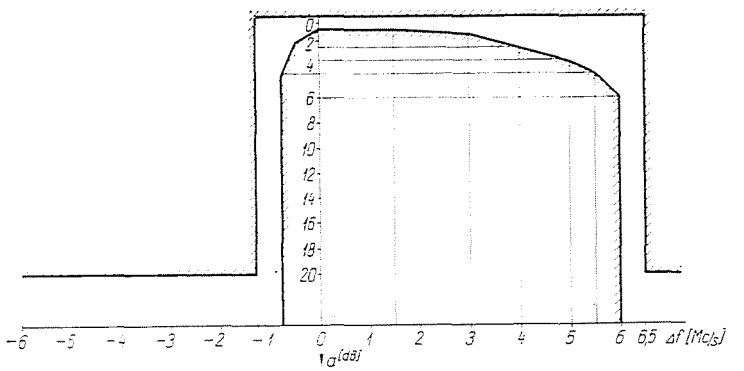

Fig. 2. Tolerance scheme of the spectrum of TV transmitters (OIRT standard)

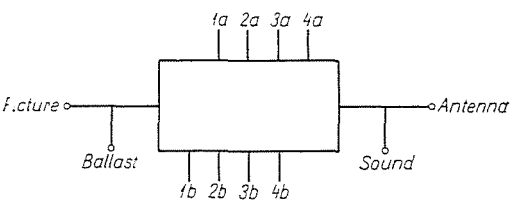

Fig. 3. Simplified schematic drawing of the filterplexer

The response curve must stay between the two given limits. The outstanding requirements are: relatively high attenuation in the rejected sideband, steep slopes at the beginning and at the end of the pass-band and low attenuation through the pass-band.

The foregoing discussion gave a short account of the working principles of the filterplexer. It was shown, that the filters connected to the bridge arms produce the desired sideband rejection, they determine the whole response curve too, and to a certain extent they take care, together with the balun transformers, of the picture-sound separation. Let us discuss the sideband rejection first (Fig. 3).

On the schematic drawing of the filterplexer the lines marked 1, 2 and 3 represent the filter pairs, which produce the sideband rejection and the overall response curve. The chief design features of these filters are: the power

should propagate possibly without any attenuation in the pass band, and should be reflected at frequencies falling in the rejected sideband.

The requirements are solved by filters type *A*, shown on Fig. 4. The two terminal networks have one series and one parallel resonant frequency besides the two extremes. The places of the series resonant frequencies are evidently chosen to fall in the rejected sideband, while those of the parallel resonant frequencies are chosen on the picture carrier.

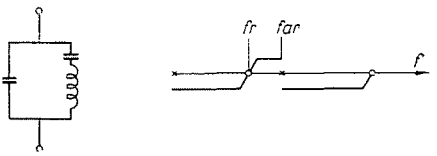

Fig. 4. The circuit of type *A* filter and its reactance curve

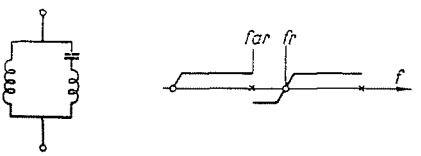

Fig. 5. The circuit of type *B* filter and its reactance curve

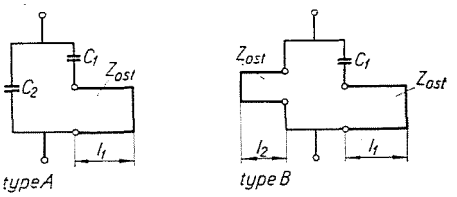

Fig. 6. The actual electric circuits of the filters

At the higher end of the pass-band the power of the sound transmitter is guided to the aerial by filters No. 4. Also these have one series and one parallel resonant frequencies, but their place along the frequency axis is naturally different from the previous ones. Namely, the series resonance is chosen to fall on the sound carrier frequency, while the parallel resonant frequency is put somewhere in the middle of the pass-band. The electrical equivalent circuit and frequency response of the sound filters (type *B* filters) are shown on Fig. 5.

The inductances and capacitors shown on Figs. 4 and 5 are not realized in their conventional lumped element form, because of the high operating frequencies. The actual electrical equivalents of the filters are shown on Fig. 6.

The capacitors are realized by metal sheets, while the inductances take the form of transmission line stubs short circuited at the ends. (The symbols

within one type of filter are the same, but C_1 and L_1 in type A and type B filters are calculated in entirely different ways!).

Let us take type A filters first. To calculate the attenuation response, one must know the reactance curve of the two terminal network, and this latter one makes it necessary to know the values of the parameters in the circuit.

The following values are chosen:

$$f_{res},\ f_{ares},\ = f_{picture} = f_p,\ \beta_p\, l_1,\ Z_{ost}\ ,$$

where f_{res} is the series resonant (or simply resonant) frequency,
f_{ares} the parallel resonant (or antiresonant) frequency,
β_p the phase constant at the frequency of the picture carrier,
Z_{ost} the characteristic impedance of the line stub.

As far as f_{res} is concerned, so far it has only been said that it falls somewhere in the rejected sideband. f_{ares}, on the other hand, has been chosen to fall on the picture carrier, which of course is a given value.

Z_{ost} is chosen to be 78 ohms, this being the characteristic impedance of transmission lines having the minimum attenuation. The choice has fallen on this value, because it is desirable to have the highest possible Q factor. For the time being let us regard these values to be given ones. Later, in the discussion, we shall return to the question of their choice. With the use of these values C_1 and C_2 can be determined by the following equations:

$$C_1 = \frac{1}{\omega_{res} \cdot Z_{ost} \cdot \mathrm{tg}\beta_{res}\, l_1} \tag{1}$$

$$C_2 = \frac{C_1}{\omega_{ares} \cdot C_1 \cdot Z_{ost} \cdot \mathrm{tg}\,\beta_{ares} \cdot l_1 - 1}\ . \tag{2}$$

These calculations are carried out for all three — 1, 2, 3 — type A filters.
In the design of type B filters the following values are chosen:

$f_{res} = f_s = f_{sound}$,
f_{ares} ,
$\beta_p\, l_1$,
$\beta_p\, l_2$,
$Z_{ost} = 78$ ohms ,

where f_s denotes the frequency of the sound carrier. With these parameters C_1 is:

$$C_1 = \frac{1}{\omega_{res} \cdot Z_{ost} \cdot \mathrm{tg}\,\beta_{res}\, l_1} \tag{3}$$

(Here, too, we shall return to the question of choice for the different values.)

According to all these the impedance values of type A and type B filters can be determined at any frequency. This is important because the individual filters are connected parallel to the bridge arms, and each filter shunts the transmission line to an extent depending on its impedance value at a given frequency.

In the following discussion the attenuation caused by a shunt reactance will be determined (see Fig. 7).

A transmission line having a characteristic impedance of Z_0 is terminated with its wave-impedance. This is shunted by a pure reactance of either $+jX$ or $-jX$. On the figure P_f denotes the forward, and P_r the reflected power.

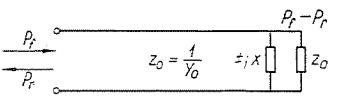

Fig. 7. A reactance connected parallel to a matched transmission line

The resulting admittance, Y_2, of the termination and of the shunt reactance is now:

$$Y_2 = \frac{\pm jX + Z_0}{\pm jXZ_0}. \tag{4}$$

The transmission line theory defines the voltage reflection coefficient:

$$\Gamma = \frac{Z_2 - Z_0}{Z_2 + Z_0} = \frac{Y_0 - Y_2}{Y_0 + Y_2}, \tag{5}$$

where Z_2 is the resulting impedance of the termination.

With the combination of Eq. 4. we get:

$$\Gamma = \frac{Y_0 - \dfrac{\pm jX + Z_0}{\pm jXZ_0}}{Y_0 + \dfrac{\pm jX + Z_0}{\pm jXZ_0}} = \frac{-Z_0}{Z_0 \pm 2jX} = \frac{-1}{1 \pm 2jX'}, \tag{6}$$

where $X' = \dfrac{X}{Z_0}$, that is the normalized impedance.

$$\Gamma = \frac{1}{\sqrt{1 + 4X'^2}} \tag{7}$$

$$|\Gamma|^2 = \frac{1}{1 + 4X'^2}. \tag{8}$$

The attenuation is defined as the ratio of the difference between the forward and reflected power and the forward power:

$$a = \frac{P_f - P_r}{P_f} = 1 - \frac{P_r}{P_f}. \tag{9}$$

Since

$$|\Gamma| = \left|\frac{U_r}{U_f}\right|; \quad \text{and} \quad |\Gamma|^2 = \frac{P_r}{P_f}, \tag{10}$$

by substituting these into Eq. 9., the attenuation results in:

$$a = 1 - |\Gamma|^2; \text{ that is in } dB:$$

$$a_{dB} = 10\log_{10}[1 - |\Gamma|^2] = -10\log_{10}\frac{1}{1 - |\Gamma|^2} \tag{11}$$

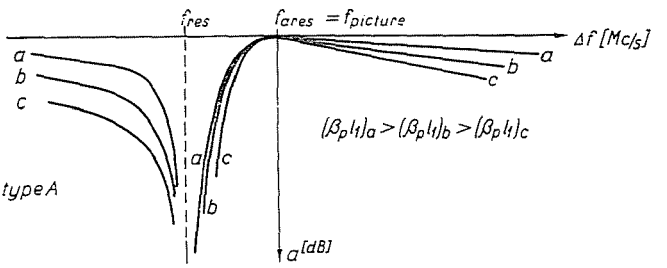

Fig. 8. Attenuation-frequency curves of type *A* filters

By using Eq. 8., we get:

$$a_{dB} = -10\log_{10}\frac{1}{1 - \dfrac{1}{1 + 4X'^2}} = -10\log_{10}\frac{1 + 4X'^2}{4X'^2} \tag{12}$$

$$a_{dB} = -10\log_{10}\left[1 + \frac{1}{4X'^2}\right]. \tag{13}$$

The attenuation can also be expressed with the voltage standing wave ratio:

$$|\Gamma| = \frac{r - 1}{r + 1}. \tag{14}$$

And so the attenuation:

$$a_{dB} = -10\log_{10}\left[\frac{1}{1 - |\Gamma|^2}\right] = -10\log_{10}\left[\frac{(r + 1)^2}{4r}\right]. \tag{15}$$

The transmission line, to which the filters are connected, can be regarded as one, terminated by its characteristic impedance. Consequently by calculation it is possible to plot the attenuation versus frequency curve caused by a filter of given parameters. (Fig. 8)

The given curves correspond to a filter having different $\beta_p l_1$ values. It can be seen, that at a given frequency the attenuation changes with the different values of $\beta_p l_1$, and by properly choosing it, one can prescribe the value of attenuation at a third frequency besides those of the f_{res} and f_{ares} frequencies.

Fig. 9. shows the attenuation curves that can be realized by the type B filters.

The response curve of the filterplexer is determined by the filters. Since the two bridge arms are symmetrically built up, it is enough to concentrate

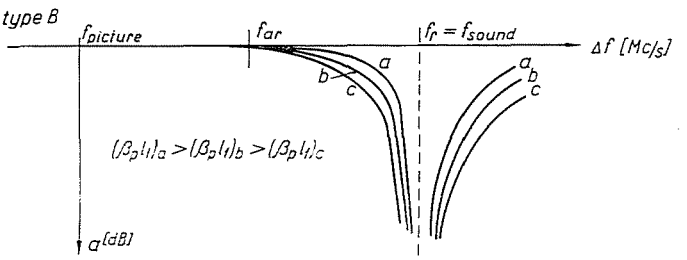

Fig. 9. Attenuation-frequency curves of type B filters

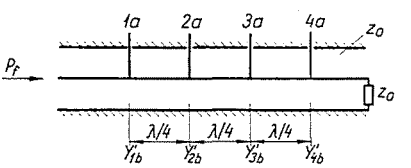

Fig. 10. Simplified schematic of one of the bridge arms of the filterplexer

on one arm only. Fig. 10. shows a section of one of the bridge arms, where the filters are represented by vertical lines ($1a$, $2a$, etc.).

Let us assume that the filters realize Y'_{1b}, Y'_{2b}, etc. normalized basepoint admittances at a given frequency. If these admittances are transformed and summed up, one after the other in the opposite direction of the propagating energy, then the basepoint of $1a$ filter is reached, where the resulting normalized admittance, Y'_r appears.

Mathematically:

$$Y'_r = Y'_{1b} + \cfrac{1}{Y'_{2b} + \cfrac{1}{Y'_{3b} + \cfrac{1}{Y'_{4b} + 1}}}. \tag{16}$$

The form of this expression follows the fact, that the individual filters are displaced a quarter wavelength from each other. Consequently at the

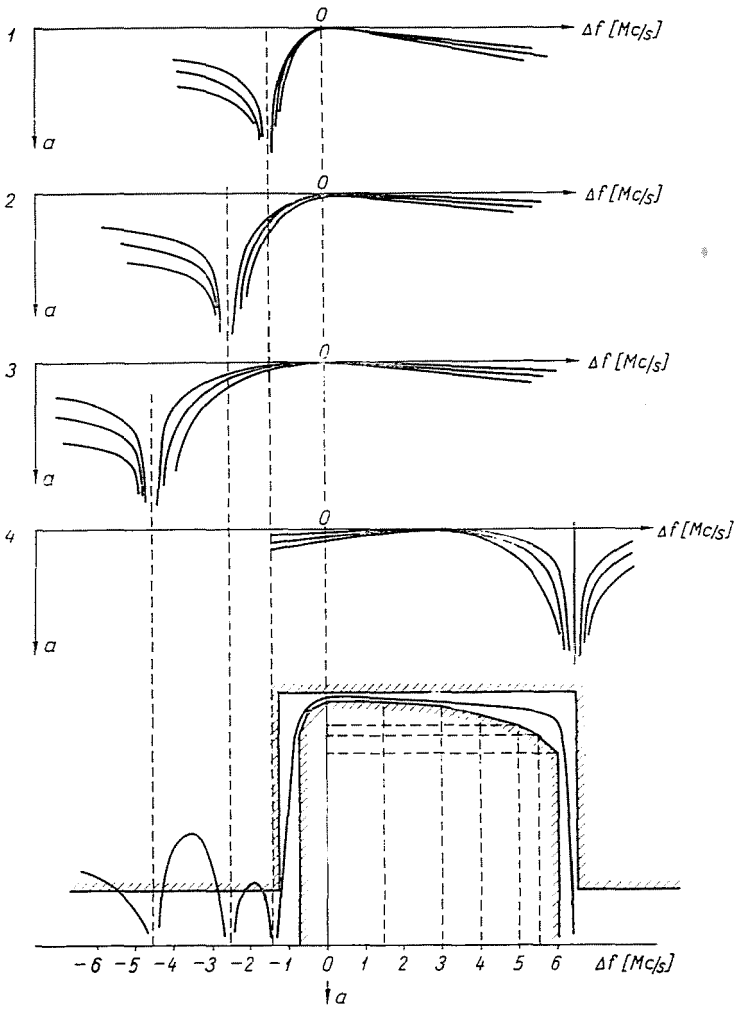

Fig. 11. The step-by-step procedure of the designing method

basepoint of filter 1*a* in the direction of the forward energy there is a Y_r' normalized admittance connected parallel to the transmission line.

If Y_r' is calculated at different frequencies in the operating band, then the attenuation can be determined with Eq. 16., and with this the attenuation versus frequency characteristics of the filterplexer is readily attained.

It was shown, however, that Y_{1b}', Y_{2b}', etc. can only be determined with the concrete values of each individual filter parameters. Besides these one must choose the resonant frequencies of the filters, the $\beta_p l_1$ values, etc.

At first try these naturally cannot be chosen in such a way as to fulfil the prescribed attenuation characteristics. In the contrary, by using the

cut-and-try method it is a very tireing work to complete the foregoing calculation procedure. Therefore, Eq. 16. — which gives the exact results — is not used at the beginning, but an approximating method, described below, is to be followed instead.

By choosing definite values, which were mentioned in the discussion of type A and type B filters ($f_{r\,s}$, $\beta_p\, l_1$, etc.) one decides the still missing parameters (C_1, C_2). After this the attenuation-frequency curves are calculated and plotted for different $\beta_p\, l_1$ values. In this way four sets of curves will correspond for the four filters. Then a choice is made of one curve out of each set of filter curves and, from now on, we shall concentrate only on these. The attenuation values are summed up at different frequencies throughout the whole band. These values are graphically represented on the tolerance scheme. Fig. 11 shows the main steps of this designing method.

It must be emphasized, that this is not an accurate designing method. This is only an approximation of the accurate results. The validity of this approximating method and its expected accuracy is dealt with in the appendix.

In this way one gets some kind of response curve. Certainly, there will be such frequencies at which this approximate attenuation curve does not fulfil the demands outlined in the tolerance scheme. From the excursions of the attenuation curve into the forbidden regions one can logically deduct the change which is necessary to make in the parameters of the individual filters (other resonant frequencies, other $\beta_p\, l_1$ parameters, etc.).

Having made these changes, the resulting curve is again approximated. By twice or three times, repeating this method, the resulting curve will usually be acceptable.

Having arrived at this point, now it is necessary to perform the exact calculations with Eq. 16. with the parameters, that the proper attenuation curve resulted with. In most cases — assuming the calculations were made in the above described order — the accurate attenuation curve will be acceptable too.

The calculations of the attenuation and base-point admittance curves of the different filters (Y_{1b}', Y_{2b}', etc.) can be considerably simplified by the use of properly calculated and plotted designing curves.

In many cases there is a need to know the reactance of a capacitor at different frequencies of a given television channel. Calculations are made much quicker, if the curve shown on Fig. 12. is plotted in proper enlargement, according to the accuracy needed. To change the capacity value from 10 pF to any other value is quite easy by means of a slide rule.

There are also quite a number of cases, in which the value of the capacitor C_1 is needed, which resonates with a stub line having Z_{ost} characteristic impedance and l_1 length at a given frequency. The curves plotted on Fig. 13 make this sort of problem rather quick to solve. From this diagramme the

impedance of the short circuited transmission line of given parameters can easily be read off, also the impedance of different capacity values within a certain extent. It is decided by concrete demands, in what region the curves are to be plotted.

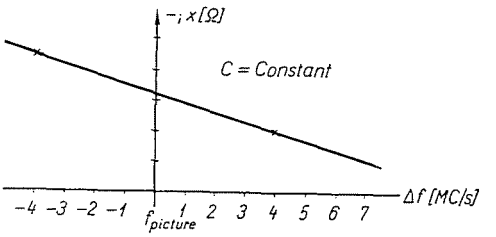

Fig. 12. The reactance-frequency curve of a capacitor

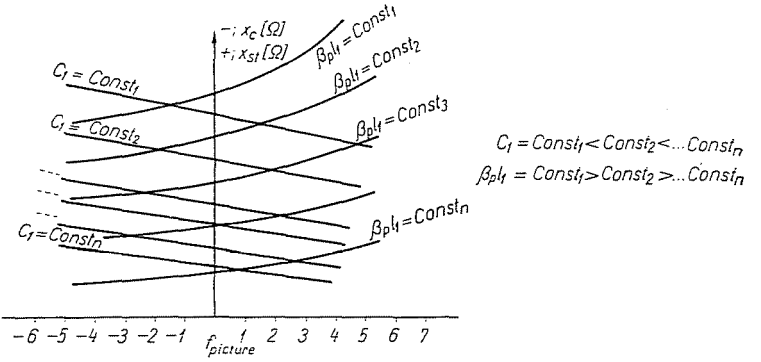

Fig. 13. The reactance-frequency curves of short circuited stubs and capacitors

2.2. *The response curve from sound transmitter to aerial*

This problem can simply be solved if based on the previous discussion. This calculation, however, should be completed only after the correct picture response curve had been attained, since all of the circuit elements are well known by then.

Since the band of the sound transmitter is relatively small (the maximum frequency deviation being ± 50 kc/s), the calculations are confined to within $\pm \Delta f = .5$ Mc/s below and above the sound carrier frequency. It was shown previously, that filters 4*a* and 4*b* resonate at the frequency of the sound transmitter. Consequently they produce practically a short circuit on the line. In the frequency band mentioned above the reactances of the filters 4*a* and 4*b* remain at such low value, that the impedances resulting at their base-points are mainly decided by them. Therefore the transformation of the reactances of the other filters can be neglected.

The attenuation versus frequency curve can be calculated on the basis of Fig. 14. At the sound transmitter input a forward power, P_f starts off towards the side branches of the balun transformer. Because of the short circuits produced by filters $4a$ and $4b$, a reflected power, P_r, propagates towards the aerial. The attenuation is given by the ratio of these two powers.

$$a = \frac{P_r}{P_f} \tag{17}$$

$$|\Gamma| = \left|\frac{U_r}{U_f}\right| \tag{18}$$

$$a = |\Gamma|^2 \tag{19}$$

$$a_{dB} = -10 \log_{10} |\Gamma|^2 \tag{20}$$

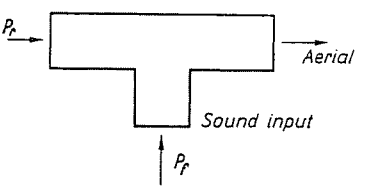

Fig. 14. Schematic circuit for the calculation of the attenuation between the sound transmitter and the aerial

By substituting Eq. 8., we get:

$$a_{dB} = -10 \log_{10} \left[\frac{1}{1 + 4X'^2}\right], \tag{21}$$

where $x' = \dfrac{X}{Z_0}$ is the value of the normalized filter impedance at a given frequency.

3. Realization of the filters and of the balun transformers

3.1. *Determination of the dimensions of the filters*

The electric data of the filters positioned on the two bridge arms have, in the previous discussion, been determined. Therefore, the following values can be regarded as given ones: (see Fig. 6)
For type A filters: C_1, C_2, l_1 and Z_{ost}:
for type B filters: C_1, l_1, l_2, and Z_{ost}.

Fig. 15. shows the actual schematic diagramme of the two types of filters. The series circuit producing the pole is realized with a capacity-tuned

cavity resonator in the case of both filters. The C_2 capacitor producing the zero in the response curve got its place just opposite to the cavity resonator for the type A filters, while for type B, the parallel inductance is realized by a short circuited stub.

The characteristic impedance of the coaxial stubs realizing the inductances is given, it is 78 ohms, the same as those of the cavity resonators. It is well known that by increasing the diameter, the Q factor of a coaxial cavity increases too. The outer diameter has been chosen to be 160 mms as a compromise between the possibilities of manufacturing and good operation charac-

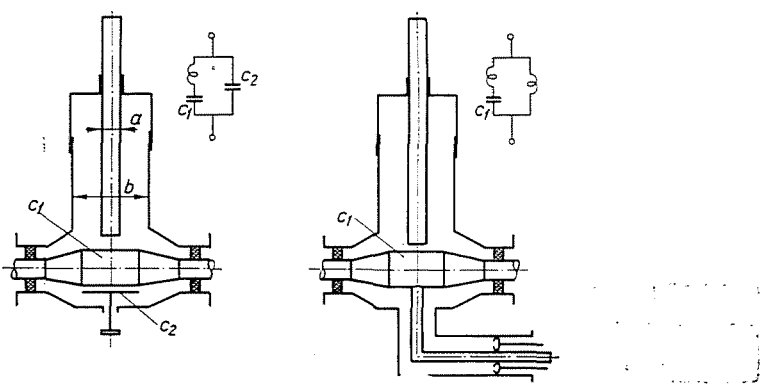

Fig. 15. The actual schematic of the two types of filters

teristics. Consequently the inner diameter can by now be calculated from the following equations:

$$Z_0 = 60 \log_e \frac{b}{a} \tag{22}$$

$$a = \frac{b}{\text{num} \log_{10} 0{,}434 \dfrac{Z_0}{60}}. \tag{23}$$

Naturally provisions are made for the exact setting of the calculated resonant frequencies by making the filters tunable. It can be seen on Fig. 15 that there are two independent means by which one can set the series resonant frequency. In this way the L/C ratio (i.e. $\beta_p l_1$) can be adjusted to the proper value besides the setting of the necessary resonant frequency.

The innermost part of the inner conductor of the filter has been dimensioned in such a way, that by air circulation the dissipated power owing to the losses can be extracted.

In the case of type A filters, the C_2 capacitor was realized with the help of a symmetric metal sheet, the distance of which from the inner conductor leading across the filter is variable by means of a screw-thread.

The parallel inductance of type B filters was realized — as has already been shown — with a short circuited stub. Its dimensions were kept low owing to the fact, that most of the losses originate in the inductance of the series circuit. In order to ensure the smallest possible room necessary for the filterplexer, these stubs were broken at 90° (see Fig. 15).

3.2. *Determination of the dimensions of the balun transformers*

There are several types of balun transformers discussed in the literature of which we have chosen the coaxially built, slotted line type. Its schematic

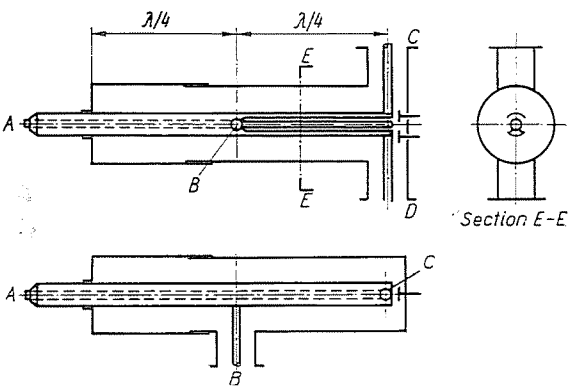

Fig. 16. Coaxially built, slotted line type balun transformer

drawing is given on Fig. 16. It consists of a threefold coaxial system. Input A is joined by a line having 50 ohm characteristic impedance to point B. At this point the diameter of the innermost conductor increases (to secure the necessary 1 : 2 impedance tranformation), while the middle conductor has two slots along its length opposite each other (to secure the necessary symmetrization). At the other end of the quarter wavelength slotted section, one half of the middle conductor is short circuited to the innermost one. Finally two outputs are provided at points C, and D for the two halves of the middle conductor.

Input B is joined to points C, and also D by a quarter wavelength transformer, while that part reaching out towards point A is short circuited. By moving this short circuit the unwanted reactances appearing at point B can be eliminated.

Since an input voltage at point A produces two voltages of opposite phase at points C and D (all three points having a characteristic impedance

of 50 ohms), the inner quarter wavelength transformer must transform 50 ohms to 100 ohms, because the two 50 ohms loads are actually connected in series.

On the other hand the voltage appearing at input B (which also has 50 ohms characteristic impedance) will produce two voltages of the same phase at points *C* and *D* (see Fig. 1). Therefore, the outer quarter wavelength transformer must transform 50 ohms to 25 ohms, because *C* and *D* are now connected parallel to each other.

These transformation demands on the whole determine the ratios of the diameters of the balun transformers. The characteristic impedance of the outer transformer is

$$Z_{0\text{outer}} = \sqrt{50 \cdot 25} = 35.4\,\Omega, \tag{24}$$

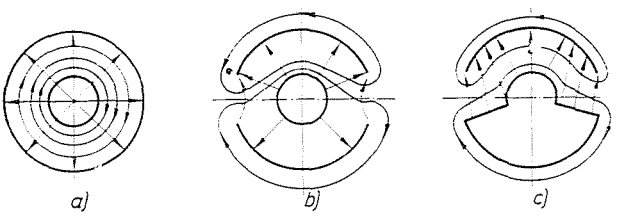

Fig. 17. Electromagnetic field-pattern in three different cross sections of the balun transformer

while that of the inner one is:

$$Z_{0\text{inner}} = \sqrt{50 \cdot 100} = 70.7\,\Omega \tag{25}$$

These equations must hold throughout the whole quarter wavelength transformer section.

The dimensions of the outer transformer can now be calculated without any difficulty, in case of the inner one, however, it is far from being so simple. That is because here besides the impedance transformation symmetrization also takes place. This latter causes a step-by-step *change* of the electromagnetic field configuration along the quarter wavelength section and the familiar coaxial field at the input (Fig. 17*a*) is replaced at the output by a field configuration given on Fig. 17*c*. The transition is continuous. Fig 17*b* shows a field pattern in a cross section somewhere between the two extremes.

According to this, the characteristic impedance of the transformer is not constant along the quarter wavelength section, so Eq. 25. may not be used for dimensioning, because it holds only for transformers having constant characteristic impedance throughout their length. The ratio of the diameters necessary for providing the 1 : 2 impedance matching has been determined empirically by measurements, which resulted as 1.8 with acceptable low tolerance.

In possession of these data the dimensioning of the whole balun transformer can be carried out. The incidental asymmetry resulting from the actual realization can be eliminated by two small plate capacitors located at the end of the balun transformer.

4. Tuning and setting up

The tuning and setting up procedure of the filterplexer is a very delicate problem at wchich the use of a proper measuring apparatus is unavoidable. We are of the opinion that the apparatus most suitable for this work is the so-called *Z—g*-Diagraph, made by ROHDE—SCHWARZ, with all its special accessories [4].

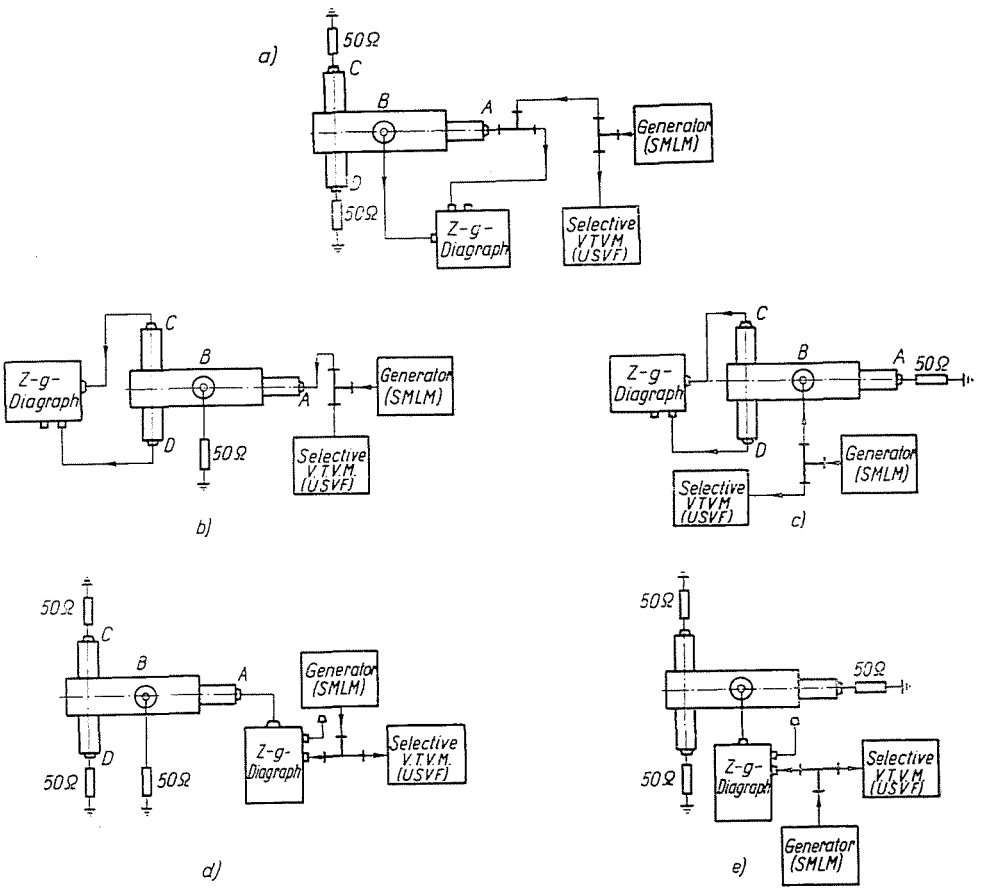

Fig. 18. The setting up of the balun transformer

a) Measurement of crosstalk attenuation between inputs *A* and *B*; *b)* Measurement of phase difference of points *C* and *D* with input at point *A*; *c)* Measurement of phase difference of points *C* and *D* with input at point *B*; *d)* Measurement of input impedance at point *A*; *e)* Measurement of input impedance at point *B*

Before the complete assemblage, the two balun transformers were separatly checked. We have measured attenuation between inputs A and B (Fig. 18 a), the phase angle between the voltages at points C and D, with the input at point A and B resp. (Figs. 18*b* and 18*c* resp.), as well as the input impedances at points A and B (Figs. 18*d* and 18*e* resp.). The symmetrizing plate capacitors were also set in at this point.

Next came the pretuning of the filters. The measuring arrangement is given on Fig. 19*a*. First the resonant frequency was set by tuning to maximum attenuation, then the antiresonance frequency, by tuning to minimum attenuation. Then on a suitable third frequency the value of the attenuation

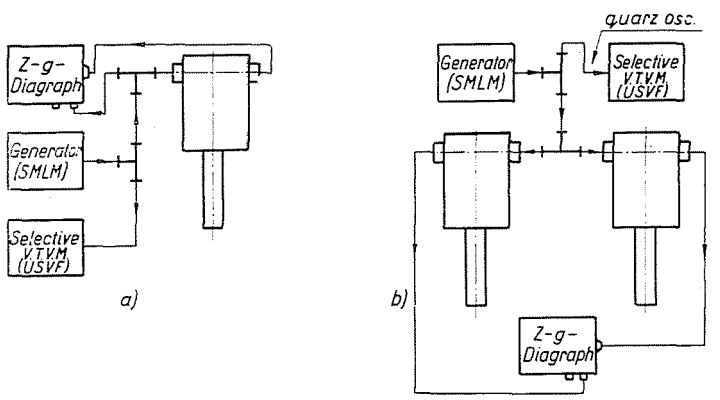

Fig. 19. Pretuning of the filters
a) Individual tuning of the filters by way of attenuation measurement; *b)* Mutual tuning of the filterpairs by way of comparative measurement

was checked. If it did not agree with the calculated (necessary) value, then having changed the L/C ratio, the above procedure was repeated, until the mesaured attenuation characteristic complied with the calculated one properly.

The next step was the mutual tuning of the filter pairs. Since the fundamental condition of the good operation of the filterplexer relies on perfect symmetry in the two bridge arms, therefore, it was absolutely necessary to bring the filter pairs to exactly the same reactance-frequency characteristics. The afore mentioned Z—g-Diagraph is especially suitable for comparative measurements and it is relatively easy to achieve this "attenuation tracking" with it [4]. The measuring arrangement is shown on Fig. 19*b*. The use of the selective vacuum tube voltmeter (USVF) is emphasized by the fact that so in this way it is possible to set the measuring frequencies with high accuracy. Namely, by previously calibrating with a quartzoscillator the signal generator can be tuned in on this same frequency with extremely high accuracy. With this method it was possible to achieve an accuracy of appr. 10^{-5}, which is especially critical when setting the poles of the two type B filters.

The first step in the course of the mutual tuning began by bringing the resonant (*i. e.* the pole) frequencies of the two filters to the same value. Then by tuning C_2 (or L_2 resp., see Fig. 6) the antiresonant frequencies were brought precisely to the same value. After this the tracking was checked on the low and high end of the band and in case of appreciable difference we made a small change in the L/C ratio of one of the filters and then repeated the above procedure. With this method it was possible to hold each filter pairs within a $\pm 3^\circ$ phase and $\pm 3\%$ amplitude tolerance.

Then followed the complete mechanical assemblage of the filterplexer. The small detuning inevitably caused during this procedure were eliminated by slightly adjusting the pole frequency of one of the filter pairs.

As a last step, a whole row of measurements were made for a final check of the filterplexer. Again the opinion was arrived at that the Z—g Diagraph is the most suitable instrument for this work because of its great variety of applications. In the whole ± 6 Mc/s band the following characteristics were measured:

Attenuation from picture input to antenna output;
Attenuation from sound input to antenna output;
Phase response from picture input to antenna output;
Phase response from sound input to antenna output;
Crosstalk attenuation from picture input to sound input;
Input impedance at the picture input;
Input impedance at the sound input.

From the curves of the phase response the envelope-delay versus frequency characteristic was also calculated, which was later used in the design of the phase corrector.

Fig. 20 shows the complete filterplexer in its operating condition. The filters being a quarter wavelength from each other are easily distinguishable from each other. The upmost filter is of type *B*, the parallel tuning inductance can clearly be seen as it is broken at right angle. The four filters of the other bridge arm can be seen on the inner side of the rack, the plane of the bridge arms being perpendicular to the axises of the filters. The two balun transformers are turned into the plane of the bridge arms, therefore, they can not be seen clearly. On the right side of the rack, on its outside, are located the switching facilities (Fig. 21) to which the picture and sound inputs, as well as the aerial output of the filterplexer are connected. The reflectometers, which continuously indicate the operating conditions, were located at the same place, their meters are positioned on the upper margin of the filterplexer rack. It is possible to continuously read from these instruments the forward and reflected powers of the picture and sound transmitters, as well as these of the filterplexer output.

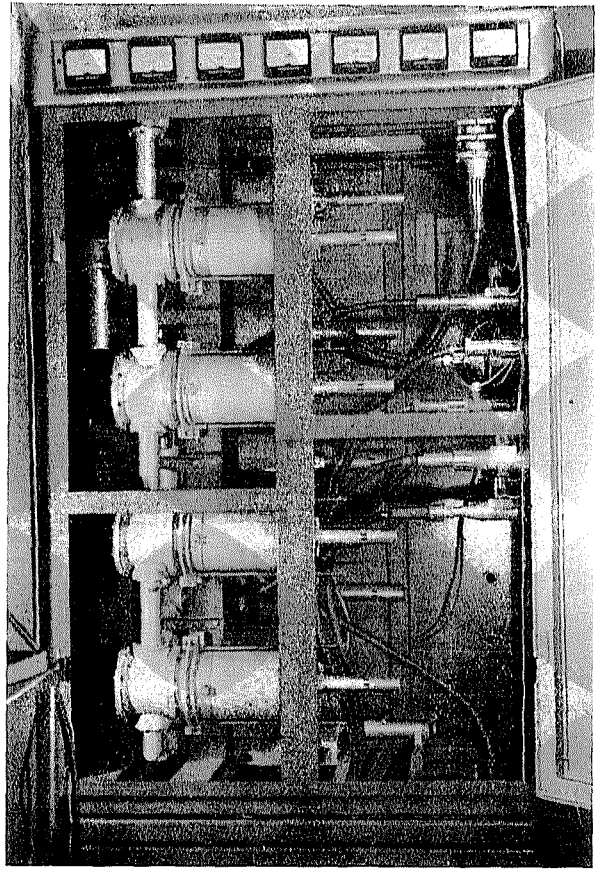

Fig. 20. Complete filterplexer designed for the channel 8 (OIRT) use

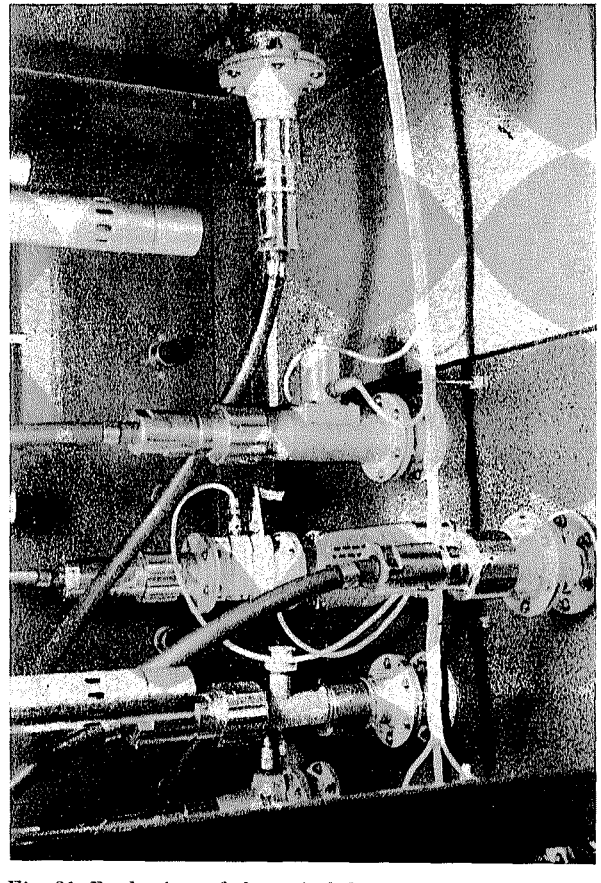

Fig. 21. Back view of the switch-board of the filterplexer with the reflectometers

5. Comparison of the calculated and measured values

In the foregoing discussion we gave a full account of all the measurements made, and now a study follows, in which a comparison is given of the measured and calculated values. This can be done only in the cases of the picture and sound response curves. The reason is, that as far as designing is concerned, only these two curves can be prescribed, where, by the way, there are concrete possibilities for determining certain values.

The same is, however, not true of the other, none the less important characteristics of the filterplexer, such as for example the change of the voltage standing wave ratio as a function of frequency or the crosstalk attenuation between the picture and sound inputs. Principally these are perfect, but in a practical realization there are several factors which have a serious influence on their values.

The most important factors are the following: the accuracy of the manufacturing methods, the assemblage and the stability of the mechanical construction. The accuracy of the manufacturing method is especially important in the case of symmetry. E. g. theoretically the pairs of filters inserted in the two bridge arms should be both geometrically and electrically symmetrical. Naturally, in practice it is impossible to realize this perfect symmetry. On the other hand, manufacturing should trend to keep the differences at the lowest possible level, while meeting the demands of the economic production. The construction, the prescribed mechanical tolerances, etc. are especially emphasized in this respect. A reasonable compromise must govern the choice of these values.

The filterplexer is very sensitive to symmetry because as we have seen, it is of the bridge type, and therefore, a difference between two units, of which we expect similar characteristics, appears all the more sharply. So for example, besides the previously mentioned filters, the excentricity difference of the two bridge arms, or the asymmetry of the balun transformers cause a change in the transformation and at the end results in a higher voltage standing wave ratio. These same undesired factors might influence the feeding of the balun transformers by changing the phase relations, which leads to a worse crosstalk attenuation value.

Even if the manufacturing is accurate, the same troubles may arise, if the assembling work is not through enough, let alone careless. It cannot be emphasized enough how important it is to conduct this stage of work, giving close attention to details.

Besides these, the mechanical stability of the assembled filterplexer is none the less important. At the end this leads up to the questions of construction. Even the most meticulous manufacturing and the most punctuate assembling cannot ensure the satisfactory operation of the apparatus. If the

fixings of the tuning elements, and generally the variable elements are not reliable, then detuning of some of the units by constant vibration might completely spoil the correct electric functioning.

In the tolerance scheme, on Fig. 22, the continuous line indicates the measured, the dotted line the calculated values. In this case the difference can be explained by two main reasons:

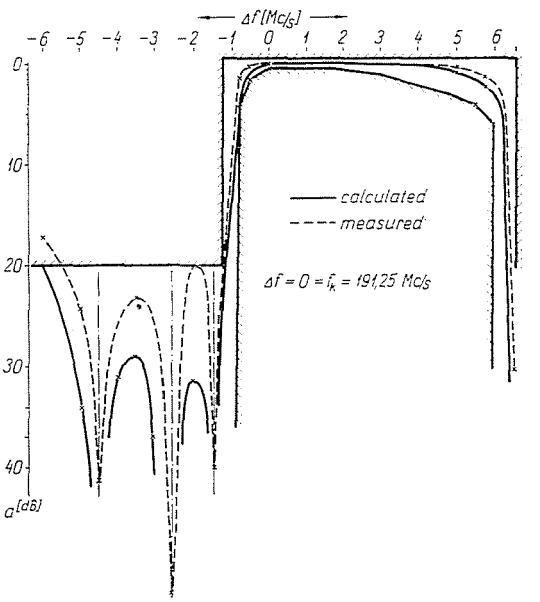

Fig. 22. Comparison of the measured and calculated values on the tolerance scheme (attenuation between picture transmitter and aerial)

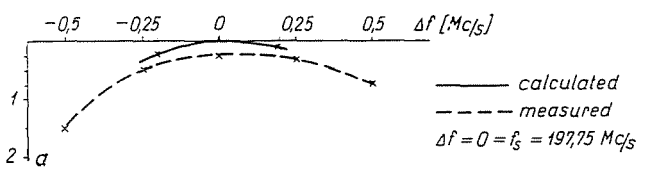

Fig. 23. Comparison of the measured and calculated values (attenuation between sound transmitter and aerial)

1. It was impossible to measure the calculated geometric tuning length of the filters from a well defined reference point, because of the transition discontinuities that are inherent in the design.

2. The Q factors of the filters are not ideally large.

The response curve of the sound transmitter is shown on Fig. 23. Here again the measured attenuation curve differs from the calculated one because

of the fundamental attenuation of the filterplexer (partly because the transmission lines are not ideal, partly because the two type *B* filters have considerable losses of their own too).

Appendix

The validity of the approximating design method described in chapter 2.1 is verified in the following.

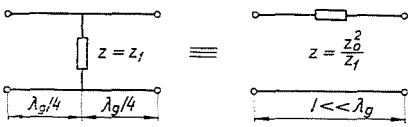

Fig. 24. Series equivalent of a parallel circuit

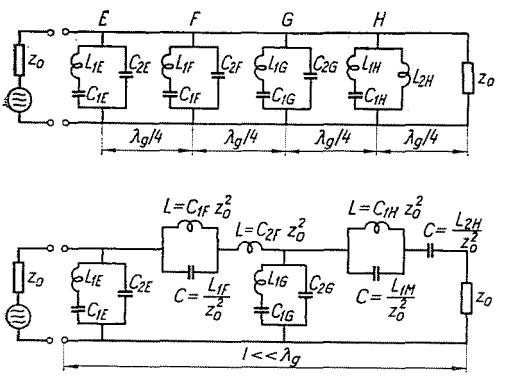

Fig. 25. Equivalent circuit of one of the bridge arms of the filterplexer

The impedance transformation features of the quarter wavelength long transmission lines are well known from the literature [5]. Hence the equivalence shown on Fig. 24. holds, where Z_1 is an arbitrary impedance, Z_0 the characteristic impedance of the quarter wavelength transmission line. With this transformation the substituting circuit of one arm of the filterplexer is shown on Fig. 25*b*. (The original circuitry is given on Fig. 25*a*.) The reactance-frequency diagrammes of the reactive two terminal networks, labelled *E*, *F*, *G* and *H* are given on Fig. 26. With the help of the series and parallel resonances the whole band is divided into five sections and for the sake of a better overlook, the transformed substituting circuit is a gain given somewhat simplified. Now let us take the sections one after the other.

Section I. — Most of this section contains the passband. Here Z_H and Z_G, as well as Z_F and Z_E have different signs, so as far as the input impedance is concerned, they more or less compensate each other's effect. So if we add

them together, according to the approximating method, this only means a neglection made toward security. It is worth noting, that the values of all four reactances are of such magnitudes that they are nearly negligible.

Section II. — This is the part between the picture carrier and the first pole. Z_H and Z_G, and Z_F and Z_E have here also different signs, therefore also in this band — like in the previous one — their summing up means a neglection made towards security.

Section III. — This is the band located between the first and second poles. It can be seen, that Z_H and Z_G compensate each other here too, while Z_E and Z_F having the same signs, increase the resulting reflection. Con-

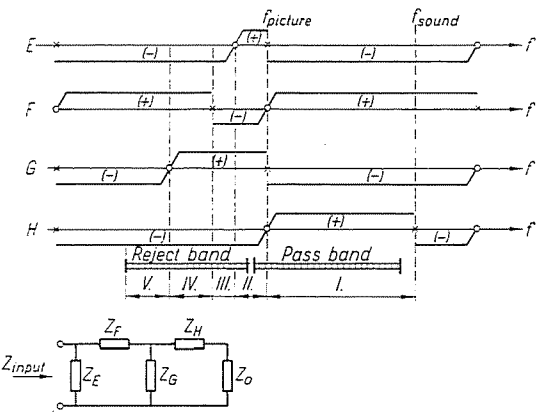

Fig. 26. Reactance-frequency curves of the reactive two-terminal networks of Fig. 25.

sequently in this case the adding up of these latter two is verified only, the magnitudes of Z_H and Z_G, however, permit them to be neglected nearly, so the sum of all four makes no appreciable difference.

Section IV. — This is the band located between the second and third poles. Virtually Z_E and Z_F, and Z_G and Z_H resp. compensate each other here, but attention should be paid to the fact that the effects of Z_F and Z_G are much greater, than those of the other two. In this way the summing up of only these two is verified.

Section V. — In the band below the third pole Z_G and Z_H have the same sign, so their effects add up, while Z_E and Z_F compensate each other. Attention is called, however, to the fact, that owing to their magnitudes Z_H and Z_G are more effective in this section.

By summing up it can be seen, that the adding up of the simple reactances in the pass band results in a worse attenuation curve, while in the reject band — especially in Section IV. — it gives a better attenuation curve than the actual one. In practice, however, by taking this into consideration

at the beginning it is possible to reach satisfactory results with the method outlined in the article. It should also be added that although in the previous study the adding up of the *impedances* was verified and not the adding up of the attenuations caused by them, — which actually was done in the approximating method — still the neglection thus made are even permissible and the deviations between the attenuation curves calculated with the approximating method and the accurate one resulting from the controle calculations are not very great.

Summary

The paper gives a full account of the new design method developed by the authors for the vestigial sideband filters and diplexers (*i.e.* filterplexers) of television transmitters. It deals in every detail with the method used for the tuning of the whole filter unit and also gives ample information about the questions of construction. At the end of the paper the data of a filterplexer designed and set up by the authors' method is compared to those of the previously calculated ones and in this way verifies the adequateness of the method.

References

1. VAN DER VORM LUCARDIE, J. A.: Philips Telecom. Rev. **126,** March (1959).
2. SCHEFFER, G.: Rohde & Schwarz Mitteil. **210,** No. 4, (1953).
3. HOLLE, J.: Frequenz, **102,** April (1959).
4. EICHACKER, R.: Rohde & Schwarz Mitteil. **75,** No. 2, (1952).
5. RAGAN, G. L.: Radiation Laboratory Series, New York, 1948. Vol. 9. 667—680.

P. FERENCZY, Budapest, XI. Stoczek u. 2., Hungary.
P. SZALAI, Budapest, XI. Petzval J. u. 31., Hungary.